Ultra High Spatio-Temporal Resolution 3D Dynamic MRI via Adaptive non-Fourier Encoding: Experimental Results

D. Mitsouras[1], F. J. Rybicki[2], A. Edelman[1], G. P. Zientara[2]

[1]EECS, Lab For Computer Science, Massachusetts Institute of Technology, Cambridge, MA, United States, [2]Radiology, Brigham And Women's Hospital, Boston, MA, United States

Introduction: Non-Fourier (NF) Encoded MRI employs spatially selective excitations in order to encode the MR signal content at the excitation step rather than using the complex exponential basis functions induced by gradients in Fourier phase encoding imaging. Some encoding bases are "best fit" to encode the contents of one FOV rather than another since the useful MR signal content of a sample has very small projections onto some subspace of the entire encoding space. This flexibility of arbitrary basis encoding, offered by NF imaging, allows one to compact the acquisition of a *k*-space [1] into its statistically significant (w.r.t. noise) components only [2], thus retaining all relevant FOV information while reducing image acquisition time. Dynamic adaptive NF encoding refers to tracking the subspace that does not meet a criteria for statistical significance through a series of changing FOV image frames. By adapting the encoding basis at each time frame, the method avoids acquisition of projections onto the "insignificant" subspace, instead focusing only on the subspace that carries the relevant FOV information. Two dynamic experiments using near-optimal encoding techniques that we present here, produced high temporal resolution 3D frames over a large FOV at very high spatial resolution at a three-fold acceleration over an equivalent Fourier encoded stack of spirals, and 4.2 over ultra-short TR steady-state methods at equivalent spatial resolution. This acceleration offered by adaptive NF encoding can be readily applied in 3D dynamic MR image guided therapies where both high spatial and high temporal resolution is required.

Theory: With RF spatial encoding, MR image acquisition is modeled as a linear system, $y=xF$, where x and y are row vectors representing the input RF and acquired data respectively, and F is a system response matrix related to the *k*-space representation of the imaged sample [3]. In particular, the row index of the matrix F ranges the *k*-space parameter(s) of the NF encoded dimension(s) while the column index ranges readout samples; all readout samples corresponding to a particular *k*-space parameter along the NF encoded dimension form one row of F. By using an arbitrary set of encoding vectors drawn from the rows of a matrix X, one acquires a response matrix Y and subsequently inverts the NF imaging equation to produce a reconstruction of the *k*-space of the sample $\hat{F} = X^{-1}Y$ and thus the image. If the rows of X are orthogonal and span a small subspace, inversion becomes a projection onto the subspace spanned by the rows of X: $\hat{F} = \{X^H X\}Y$. If X has k rows and M columns, i.e., F has M rows, the acquisition of $\hat{F}$ is completed in k encoding steps rather than M phase encode steps. That is, an acceleration of M/k is obtained over encoding with the oblivious Fourier basis. When a dynamic series of images is desired, the contents of the FOV at time t_i, F_i, are similar to the contents at the previous time step, F_{i-1}. Thus a basis that is best fit for F_{i-1} is likely close to best fit for F_i. In this work we use X drawn from the Singular Value Decomposition of F_{i-1}, although methods such as DATUM [4] can guarantee better adaptive bases. The number of SVD encoding vectors, k, can be chosen based on the SNR of the imaging method [2], ensuring that no significant information is lost. Finally, both parallel imaging and UNFOLD methods are compatible with NF encoding and can be implemented to further accelerate acquisition, as in Fourier basis imaging.

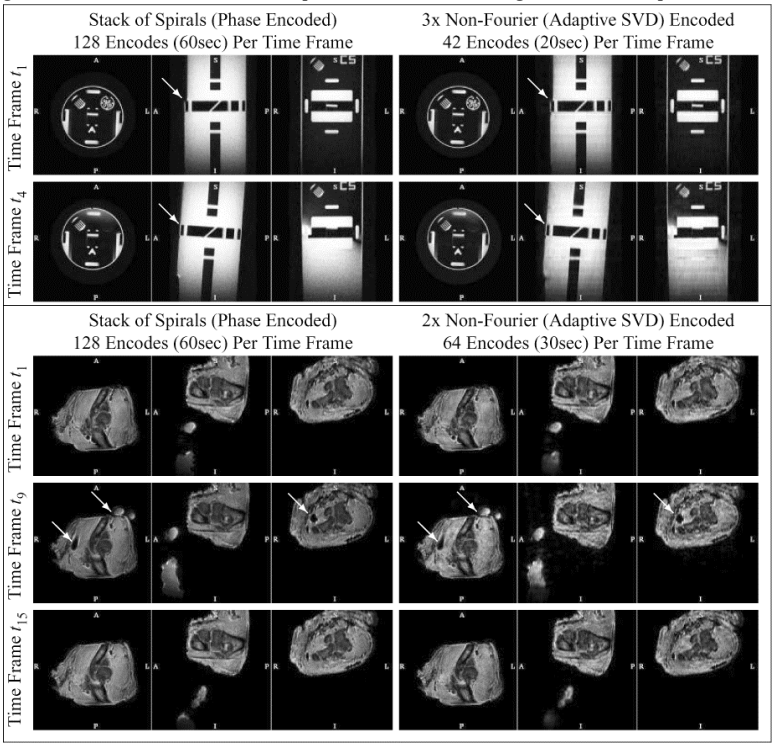

Methods & Results: All experiments were performed using a gradient recalled echo 2D spiral/1D non-Fourier encoded pulse sequence [2] running on a commercial 1.5T MR scanner (Signa LX EchoSpeed, GE Medical Systems, Milwaukee, WI). TR was 60msec, and an 8 interleave 256-by-256 spiral acquisition was used. In both experiments, the spiral ranged the A/P and L/R axes, while the NF encoded axis was I/S (as was the axis of phase encoding for the stack of spirals). Acquisition of each time frame involved imaging the sample twice, once using a phase encoded stack of spirals and once using NF encoding. No information was shared between the two sequences; the Fourier sequence was acquired for comparison. The NF encoded imaging cycle consisted of using a small set of encoding vectors to acquire time frame t_i, except the first time frame (i=0), which was acquired using the full Hadamard basis. The rank reduced (i>0) raw acquisition data was then used to compute a new reduced set of near-optimal NF encoding vectors. Once those spatial encodes were computed (2-3sec), a change of the sample was made in the FOV. The encoding vectors (computed prior to the change) were then used to acquire the new, changed FOV time frame t_{i+1}. A stack of spirals was also acquired at that time, before continuing on to the next time frame's imaging cycle. In the first experiment, a cylindrical doped water phantom was placed with its long axis along I/S (the axis of NF encoding). Between the acquisition of each 3D imaging frame t_i, which was acquired using spatial encodes computed to near optimally encode the previous frame (t_{i-1}), the phantom was rotated appx. 3 degrees about the L/R axis, maximally changing the contents along the NF encoded dimension (axial planes). The first and 4th frames are shown in the top figure. FOV was 16(L/R)x16(A/P)x27cm(I/S), and each NF encoded time frame was acquired using 42 encoding vectors, versus 128 phase encodes for the stack of spirals. Thus imaging time per frame was 20.16sec for each NF frame (8 interleaves per encode, 42 encodes) and 61.44sec for the stack of spirals. An equivalent resolution 2D or 3D steady state acquisition, with a TR of 2.6msec (current limit for a 128-by-128 acquisition on our system) would have required 85.2sec. Three-plane cuts from the reconstructed volume are shown from both the Fourier (left) and adaptive NF (right) reconstructions. The same planes are shown in all subfigures (Axial at S14, Sagittal L20 and Coronal A4). All observed change is entirely due to movement of the sample in the FOV. For example, the shifting of the doped water to fill empty volumes while the air bubble shifts to the A-I corner is successfully observed (see arrows). Had 42 phase encodes been used for acquisition, the resulting 6.4mm resolution along I/S would have been insufficient to entirely observe the detail. In the second experiment (bottom figure), a hand phantom (glove filled with gel) was moved towards an animal tissue phantom. Subsequently a 22G biopsy needle was inserted into and removed from the tissue, and finally the hand was removed from the FOV. All parameters were as in the previous experiment, except an FOV of 22(A/P)x22(L/R)x27cm(I/S) was used.

Conclusion: Two 3D experiments, one demonstrating the properties of adaptive NF encoding and the second simulating an image guided therapy, illustrate the successful depiction of the dynamics at high spatial resolution and a greater than three-fold temporal acceleration.

Acknowledgments: This research was supported in part by NIH NCI R01-CA78299, NCI P01-CA67165, NCI T32-PA-00-103, an Edgerly Science Partnership Award and an Oxygen Alliance grant. FJR was supported by NIH K23-EB882, and a Whitaker Foundation grant.

References: [1] Zientara GP et. al. *MRM*, 32:268–274 (1994)

[2] Mitsouras D, et. al. *Proc. 11th ISMRM*, Toronto, Canada, 1012 (5/2003).

[3] Panych LP et. al. *IJIST*, 20:143–150 (1999).

[4] Hoge SW et al. *Proc. 10th ISMRM*, Hawaii, USA, 2380 (5/2002).